N84 10152

CATALYTIC SURFACE EFFECTS ON SPACE SHUTTLE THERMAL PROTECTION SYSTEM DURING EARTH ENTRY OF FLIGHTS STS-2 THROUGH STS-5

David A. Stewart and John V. Rakich
Ames Research Center, Moffett Field, California

and

Martin J. Lanfranco
Informatics, Inc., Palo Alto, California

SUMMARY

This paper describes an on-going "OEX" catalytic surface effects experiment being conducted on the Space Shuttle. The catalytic surface effects experiment was performed on four of the five flights of Columbia. Temperature-time histories and distributions along the midfuselage and wing of the orbiter were used to determine the surface catalytic efficiency of the baseline HRSI. Correlation parameters are shown that allow the comparison of all flight data with predictions from the design trajectory 14414.1. These data show that the catalytic surface efficiency increased and surface emittance decreased as a result of contaminants during the five flights of the Space Shuttle.

INTRODUCTION

The possibility of reduced heating of the Shuttle orbiter during atmosphere entry because of noncatalytic surface effects has generated great interest since the first Shuttle flight, when surface temperature was found to be lower than expected. Noncatalytic surface effects for the Shuttle were previously predicted from computations and arc-tunnel tests (ref. 1) and were later confirmed (ref. 2) by data from flight STS-2. With present experience from the first five Shuttle flights, more definitive conclusions can now be made regarding noncatalytic surface effects.

The catalytic surface effects (CSE) "OEX" experiment was designed to determine if the low catalytic efficiency of the coating on the heat shield tiles would persist at flight conditions. The CSE experiment was conducted on four of the five flights of Columbia. This on-going experiment uses baseline high-temperature reusable surface insulation (HRSI) tiles located along the midfuselage and wing of the orbiter. The HRSI tiles are covered with a reaction cured glass (RCG) coating to provide emittance control and ease of handling (ref. 3). Development flight instrumentation (DFI) was used to measure surface temperature and pressure without impacting the Space Shuttle operations. A catalytic overcoat of black iron cobalt chromia spinal in a polyvinyl acetate binder was sprayed onto selected tiles (ref. 1). Measured surface temperatures obtained from tiles with and without the catalytic overcoat were compared with theoretical predictions using the reacting boundary-layer computation of Rakich and Lanfranco (ref. 2). High-temperature surface properties obtained from ground-test facilities for the RCG glassy surface and catalytic overcoat were used along with individual trajectory data to perform the computational

PAGE 826 INTENTIONALLY BLANK

PRECEDING PAGE BLANK NOT FILMED

analysis to define each flight experiment. Temperature-time histories and distributions along the midfuselage and wing of the orbiter were used to determine the surface catalytic efficiency of the baseline HRSI. This paper describes results (lessons learned) from a collection of flight data obtained from flights STS-2 through STS-5. The data include optical properties and surface temperatures that are used to define the surface catalytic efficiency of the Space Shuttle thermal protection system (TPS). A correlation parameter and a normalized surface temperature are introduced that allow the comparison of all flight data with a prediction obtained from the design trajectory 14414.1.

SYMBOLS

C_H	heat-transfer coefficient
C_p	specific heat
H_w	wall enthalpy
I_r	total enthalpy
k_w	reaction-rate constant
$\bar{L}$	Lewis number
L	orbiter length, 32.77 m
M	Mach number
P	pressure
q	heat flux
R	Reynolds number
T	temperature
t	Earth entry time, from 122 km
V	velocity
X	axial distance from nose of orbiter
Y	spanwise distance from orbiter centerline
α	angle of attack
δ	tile thickness
σ	Stefan-Boltzmann constant
ϵ_{TH}	total hemispherical emittance
ρ	density

ϕ roll angle

θ sweep angle

Subscripts:

e boundary-layer edge

0 stagnation condition

w wall condition

∞ free-stream condition

FLIGHT EXPERIMENT

The catalytic surface effects experiment consisted of two phases. The first phase was completed with STS-5. It used tiles with single surface thermocouples. The tiles were sprayed with a catalytic overcoat; temperatures were compared with those of nearby uncoated tiles. Tile locations for the first phase were at $X/L = 0.15$ and $X/L = 0.4$ for STS-2 and $X/L = 0.3$ and $X/L = 0.4$ for STS-3. Before flight STS-4, tiles located at $X/L = 0.1$, 0.15, 0.2, 0.3, and 0.4 along the midfuselage were sprayed with the catalytic overcoat; however, no entry heating data were obtained from the flight because of a data system malfunction. Tiles located at $X/L = 0.1$, 0.15, 0.2, 0.3, and 0.6 along the midfuselage and those at $X/L = 0.76$ and $X/L = 0.82$ along a 60% semispan on the wing were also sprayed with the catalytic overcoat for flight STS-5. For the same flight, a strip, 1.52 m by 0.22 m, along the midfuselage between $X/L = 0.35$ and $X/L = 0.4$ was sprayed with the catalytic overcoat (fig. 1). The catalytic overcoat was sprayed with an air brush to a thickness maintained at approximately 0.005 cm. A plastic sheet masked off the surrounding tiles (fig. 2).

The second phase, which is in the development stage, requires tiles that are constructed with multiple surface thermocouples. The catalytic overcoat will be sprayed onto one of several tiles to define the shape of the heat pulse during Earth entry of the orbiter.

POST-FLIGHT EVALUATION

Flight Photographs

Pre- and post-flight STS-5 photographs of tiles with the catalytic overcoat are shown in figures 3 and 4. The preflight photograph (fig. 3) shows (looking toward the nose) the tiles on the strip and at $X/L = 0.3$ and $X/L = 0.2$. The post-flight photographs (fig. 4) show that the catalytic overcoat on the nose wheel door ($X/L = 0.1$), fuselage ($X/L = 0.6$), and wing ($X/L = 0.76$ and $X/L = 0.82$) of the orbiter remained intact. The catalytic overcoat on the strip was eroded from the corner of two tiles along its edge during flight. However, the major portion of the overcoat remained on the surfaces. A change in color of the RCG surface from black to gray can be observed on the midfuselage and on the wing of the vehicle, indicating possible surface contamination. Visual inspection showed that the color change was

not noticeable after STS-3, but it became more pronounced after STS-4 and STS-5. However, a color change was observed on the body flap after earlier flights. Possible sources of contamination are the gap fillers in the nose wheel door and metallic sensors located along the midfuselage between $X/L = 0.1$ and $X/L = 0.2$ (fig. 5). Contaminants from these sources have been identified as Fe_2O_3, SiO_2, and Cr_2O_3 (Flowers, O. L., private communication, 1982).

Chemical Analysis

Chemical analyses were conducted on the surface of two tiles removed from locations $X/L = 0.138$ and $X/L = 0.4$ on the orbiter after flight STS-5 (Dr. Daniel B. Leiser, private communication, 1983). Analyses of the surfaces were performed using X-ray diffraction (XRD) and a scanning electron microscope with an X-ray fluorescence attachment. The X-ray fluorescense analysis attachment, an energy dispersive X-ray analysis (EDX) unit, was used to obtain qualitative chemical analysis data of the coating surface; a description of the unit is given in ref. 4. Post-flight STS-5 XRD analysis of the RCG coatings showed the presence of cristobalite on the surface. In addition, X-ray fluorescence analysis showed the presence of aluminum, silicon, sodium, and magnesium on the surface of the two tiles. The aluminum, probably in the form of alumina, is attributed to by-products deposited from the burning solid rocket fuel during launch. The other elements are commonly found in sea salt. Sea salt tends to increase the reaction-rate constant because of its effect on ion mobility and viscosity of the borosilicate glass, and alumina decreases the emittance.

Surface Properties

Two important surface properties that determine surface temperature on the heat shield are (1) the reaction-rate constant and (2) total hemispherical emittance. The reaction-rate constants for the RCG coating and catalytic overcoat surfaces were obtained from experiments conducted in the Ames Research Center Aerodynamic Heating Facility. The reaction-rate constant for baseline RCG is shown in figure 6. The reaction-rate constant varied from roughly $k_w = 25$ cm/sec to $k = 100$ cm/sec for most of the area over the midfuselage where the catalytic surface effects experiment was being conducted. For simplicity in the reacting boundary-layer computation the reaction-rate constant was assumed to be constant at $k_w = 100$ cm/sec. After flight STS-2 experiments using a microwave cavity generated nitrogen plasma on pieces of RCG covered tiles showed no change in the reaction-rate constant. Post-flight STS-5 experiment also showed no change in the reaction rate-constant for the RCG coating.

The total hemispherical emittance for both surfaces is plotted in figure 7. The preflight total hemispherical emittance of both surfaces is very similar over the temperature range of interest (figs. 7(a) and 7(b)). Taken at room temperature, the total hemispherical emittance for both surfaces was calculated from spectral, hemispherical reflectance data obtained using a Beckman model DK-IA (wavelength range 0.3 μ to 2.3 μ) and a Willey model 318 (wavelength range 2.0 μ to 15 μ) spectrophotometer, respectively. Spectral hemispherical emittance data for the RCG surfaces are plotted in figure 7(c). Figure 7(d) shows a comparison of the total hemispherical emittance calculated from spectral hemispherical reflectance data and values obtained from arc-jet tests. The arc-jet data were obtained from disks tested in an arc-plasma airstream using measurements of the radiant flux and surface temperature. The radiant heat flux was measured using a radiometer and the surface temperature with a surface thermocouple (platinum-platinum/13% rhodium) and pyrometer

(wavelength = 0.9 μ). Post-flight STS-5 total hemispherical emittance calculated from reflectance measurements is shown in figure 7(a). Post-flight STS-5 data were obtained from two tiles removed from the midfuselage at locations X/L = 0.138 and X/L = 0.4 adjacent to the baseline reference tiles. These data show less than 5% decrease in the total hemispherical emittance of the RCG coating after STS-5.

Computations

The reacting boundary-layer computation uses dynamic pressure, velocity, and angle of attack from the flight trajectory and calculated wall pressure in addition to the above described surface properties, to predict surface temperature on the orbiter TPS during Earth entry. The wall pressure-stagnation pressure ratio was calculated using an inviscid nonequilibrium real-gas solution. Typical pressure ratios are plotted for several locations along the midfuselage of the orbiter for flight STS-3 (fig. 8). Agreement between the flight data and predictions is good for all locations except X/L = 0.1 where the prediction was high. The difference in the measured and calculated pressure is attributed either to a local disturbance of the boundary layer or possible leakage of the pressure line from the surface of the tile to the transducer. Boundary-layer calculations of the radiation equilibrium temperature were performed for equilibrium and reacting flows. The calculated heating for STS-3 is shown for two surface locations (X/L = 0.15 and X/L = 0.4) along the midfuselage of the orbiter (fig. 9). Shown on the figure are the calculated wall pressure histories. The flow is assumed to be laminar in the vicinity of the experiment for the majority of the Earth-entry trajectory, when surface catalytic effects are important. Transition to turbulent flow was assumed to occur late in the Earth entry of the orbiter (~1200 s). The computations show that a reacting flow resulted in a 34-40% reduction in the heat-transfer rate at X/L = 0.15 and 25% reduction at X/L = 0.4 for a substantial portion of the heating history. The effect of this temperature reduction on heat-shield thickness was evaluated. A one-dimensional model calculation using a modified charring material ablator (CMA) program shows that for reacting flow the tile thickness can be reduced by greater than 22% at X/L = 0.15 and greater than 6% at X/L = 0.4 and still meet Shuttle design requirements.

RESULTS AND DISCUSSION

Flight data for STS-2 and STS-3 are compared with the computations and shown in figure 10. The surface-temperature distribution along the midfuselage was calculated for equilibrium and reacting flows at an entry time of 650 s. The boundary-layer analysis predicts a discontinuous rise in temperature on the test tile with catalytic overcoat. The temperature rise goes above the equilibrium value because of the sudden release of the energy of dissociation. The agreement between theory and data is good at the forward location X/L = 0.15 for STS-2. The low temperature at X/L = 0.4 can be attributed to the removal of some of the catalytic overcoat on this tile during STS-2 entry to Earth. Better agreement between flight data and theory was observed on STS-3. Some of the temperature data points are off the centerline and those should be a little higher than those on the centerline. These flight data show that the surface temperatures on the baseline HRSI tiles are consistently below the equilibrium computation (13% to 35%), and the data from the test tiles are above equilibrium.

Data Correlation

To compare data from each flight, a normalized surface temperature and a correlation parameter had to be determined. The normalized surface temperature ($\bar{T}$) was derived from the well-known expression for flat-plate heating with dissociated gas flow (ref. 5):

$$-q_w = C_H \rho_e V_e (I_e - H_w) \left[\frac{(C_{p_f})_{av}}{(C_p)_{av}} (1 - \bar{L}) + \bar{L} \right]^{1/3} \tag{1}$$

and assuming

$$\bar{L} = 1, \quad q = \varepsilon_{TH} \sigma T_w^4$$

$$\bar{T} = \frac{T_w}{\left[\frac{\rho_\infty V_\infty^3}{2r} \right]^{1/4}} = \left[\frac{C_H}{\varepsilon_{TH}} \frac{\rho_e V_e}{\rho_\infty V_\infty} \right]^{1/4} \tag{2}$$

The hypersonic viscous interaction parameter ($M_\infty / \sqrt{R_\infty}$) was found to be a correlation parameter relating equivalent flight conditions during each trajectory. To illustrate the validity of this parameter, heat-transfer coefficients for equilibrium and reacting flows were calculated for the design trajectory 14414.1 and plotted as a function of the hypersonic, viscous interaction parameter (fig. 11). Calculated values of the heat-transfer coefficient C_H obtained from trajectories STS-2 through STS-5 were compared with values from the design trajectory 14414.1. Excellent agreement was obtained between values obtained from the flight and design trajectories. Since the normalized surface temperature is proportional to C_H, it follows that the flight data also can be directly compared with the design trajectory 14414.1 prediction using the hypersonic viscous interaction parameter.

Normalized surface temperatures for several locations along the midfuselage of the orbiter (X/L = 0.15, X/L = 0.3, and X/L = 0.4) were plotted against the correlation parameter (fig. 12). The predictions included values for equilibrium and reacting flows. Figure 12 shows values of the average surface-temperature rise across the tiles with the catalytic overcoat (short dashed line). In general, good agreement between the flight data and the predictions was obtained. During STS-2, the low temperature measurement at X/L = 0.15 on the baseline RCG coating occurred with a thermocouple that failed a little over halfway through the entry to Earth of the orbiter. The low-temperature measurement for the coated tile at X/L = 0.4 during STS-2 occurred as a result of the loss of some catalytic overcoat.

The correlation parameter for all orbiter flights is plotted as a function of the time of entry to Earth from 121,920 m (fig. 13). Also, angle of attack and roll angle are shown on the figure. These calculated parameters ensure that the flight data are compared at similar flight conditions without large deviations in angle of attack or roll angle. Four cases of laminar flow conditions were chosen to compare normalized surface-temperature distributions along the midfuselage and wing with predictions using the design trajectory 14414.1 (figs. 14 through 16).

Midfuselage Heating

Figures 14(a) through 14(d) show normalized surface temperature as a function of distance along the orbiter midfuselage centerline. Boundary-layer computations are shown for equilibrium and reacting flows. The flight data on figure 14 include off-centerline corrections using the solutions outlined in reference 6. Good agreement between STS-2, STS-3, and the prediction using the reacting flow is shown for all four cases. The flight data from STS-5 appear high for the baseline RCG coating and low for tile surfaces with the catalytic overcoat. The difference between these data cannot all be accounted for by the 5% reduction in the total hemispherical emittance measured after flight STS-5. The difference between the STS-5 data and the prediction is attributed to an increase in k_w for the RCG surface coating. The lower surface-temperature measurements at $X/L = 0.2$ during STS-5 and higher surface-temperature measurements at $X/L = 0.3$ during STS-3 on the tiles with the catalytic overcoat cannot be explained at this time. These data show that the surface catalytic effect on surface temperature decreases with decreasing Mach number and with increasing distance along the midfuselage centerline of the orbiter. In figure 14(b), $M_\infty/\sqrt{R_\infty} = 0.0184$ includes a prediction for a reacting flow and reaction-rate constant that varied with temperature (see fig. 6). The normalized temperature-distribution prediction was in close agreement with the flight data from STS-2 and STS-3 along the midfuselage centerline.

The temperature at $X/L = 0.4$ on STS-5 is lower than the peak overshoot value because of the long (1.5 m) run of catalytic overcoat. However, that temperature is still above equilibrium, which is in agreement with the theory.

The temperature distribution along the midfuselage centerline of the orbiter was calculated using post-flight STS-5 total hemispherical emittance and assuming a reaction-rate constant $k_w = 200$ cm/sec for the RCG glass coating (fig. 15). Included on the figure are computations for equilibrium flow and a reacting flow with $k_w = 100$ cm/sec for the RCG glass coating. All computations were made for test point $M_\infty/\sqrt{R_\infty} = 0.0304$. The calculations using STS-5 post-flight total hemispherical emittance and increased reaction-rate constant during STS-5 agree well with the flight data. A substantial heat reduction below the equilibrium value still occurs at $X/L < 0.2$. However, at $X/L > 0.2$ the reduction in heating to the surface of the tiles is less between the reacting and equilibrium flows.

Wing Heating

To test for possible noncatalytic effects on the windward side of the wing, two tiles along the 60% semispan ($Y/L = 0.60$) were sprayed with the catalytic overcoat. This test was necessary because of uncertainty as to the origin of streamlines wetting the wing surface. If the streamlines originate at the nose of the Shuttle, the flow should be close to equilibrium because of the large distance from the nose and the results observed at $X/L = 0.6$ along the midfuselage. On the other hand, if the wing streamlines pass through the wing-leading-edge shock, then the flow has greater possibility of being out of equilibrium, and lower noncatalytic heating can occur. Streamlines from wind-tunnel tests suggest the latter possibility.

Because of the difficulty in exactly computing the wing flow field, simple two-dimensional strip theory was used to analyze the wing heating. Cutting the wing at $Y/L = \text{constant}$ yields a section shape that can be approximated by a blunted flat plate. For heating computations, the boundary layer is assumed to flow two dimensionally over the plate, starting approximately on the stagnation line on the wing

leading edge. The surface pressure is approximated with a Newtonian type of pressure distribution. Thus, the wing pressure was approximated by:[1]

$$\frac{P_w}{P_0} = \cos^2(\theta - \theta_0) \tag{3}$$

where, due to the wing sweep, $\theta_0 = 50°$ for $\alpha = 40°$ and P_0 is the normal shock stagnation pressure. The pressure and normalized surface temperature are shown in figure 16. The heating computation included a correction for boundary layer swallowing effects (ref. 2).

The Newtonian pressure approximation is, of course, constant on the flat part of the wing, but agrees reasonably well with the level of flight data, STS-3. The pressure data decrease with distance as the overpressure caused by the blunted leading edge decays toward the flat-plate value.

Figure 16 shows normalized surface-temperature predictions as a function of distance along a 60% semispan located on the wing of the orbiter. The normalized surface temperatures show peaks at $X/L = 0.76$ and 0.81, where the tiles are coated. We note that the data for the coated tiles show a significant rise over the uncoated tiles indicating a significant noncatalytic effect. The theory overpredicts the catalytic overshoot but is in fair agreement with the baseline tiles. As with the centerline data, there seems to be a slight rise in temperature of the baseline tiles for flight STS-5. This tendency has been discussed earlier. In summary, the wing heating is reasonably well predicted by simple two-dimensional strip theory.

CONCLUDING REMARKS

Lessons learned from the catalytic surface effects experiment on four STS Columbia flights flown are listed below.

1. Low surface catalytic efficiency of the RCG-coated baseline tiles results in lower heating during Earth entry for early flights of the orbiter.

2. Decrease in surface temperature on the HRSI because of its catalytic surface efficiency was less with distance along the orbiter midfuselage and Earth entry time.

3. Total hemispherical emittance of RCG coating decreased with number of flights.

4. Results indicate that surface catalytic efficiency (reaction-rate constant) of the RCG coating increased with number of flights.

5. Thermal response predictions can be made from ground-test data, design trajectory, and reacting boundary-layer computation.

---

[1]We note that equation (3) is not applicable at the wing leading edge because wing sweep reduces the pressure there, but it is adequate to start the boundary-layer computation.

6. Correlation parameter and a normalized surface temperature allow the comparison of data from several flights with predictions along the midfuselage and wing from the design trajectory 14414.1.

7. Flight data confirm the noncatalytic surface effects on the wing.

REFERENCES

1. Stewart, D. A.; Rakich, J. V.; and Lanfranco, M. J.: Catalytic Surface Effects Experiment on the Space Shuttle. AIAA Paper 81-1143, Palo Alto, Calif., 1981.

2. Rakich, J. V.; Stewart, D. A.; and Lanfranco, M. J.: Results of a Flight Experiment on the Catalytic Efficiency of the Space Shuttle Heat Shield. AIAA Paper 82-0944, St. Louis, Mo., 1982.

3. Goldstein, H. E.; Leiser, D. B.; and Katvala, V.: Reaction Cured Borosilicate Glass Coating for Low-Density Fibrous Silica Insulation. Borate Glasses, Plenum Corp., New York, 1978, pp. 623-634.

4. Leiser, D. B.; Stewart, D. A.; and Goldstein, H. E.: Chemical and Morphological Changes of Reusable Surface Insulation Coatings as a Function of Convectively Heated Cyclic Testing. NASA TM S-2719, 1972.

5. Dorrance, W. H.: The Dissociated Laminar Boundary Layer. Viscous Hypersonic Flow, McGraw-Hill Book Co., New York, 1962, pp. 69-101.

6. Rakich, J. V.; and Lanfranco, M. J.: Numerical Computation of Space Shuttle Laminar Heating and Surface Streamlines. Journal of Spacecraft and Rockets, vol. 14, no. 5, May 1977, pp. 265-272.

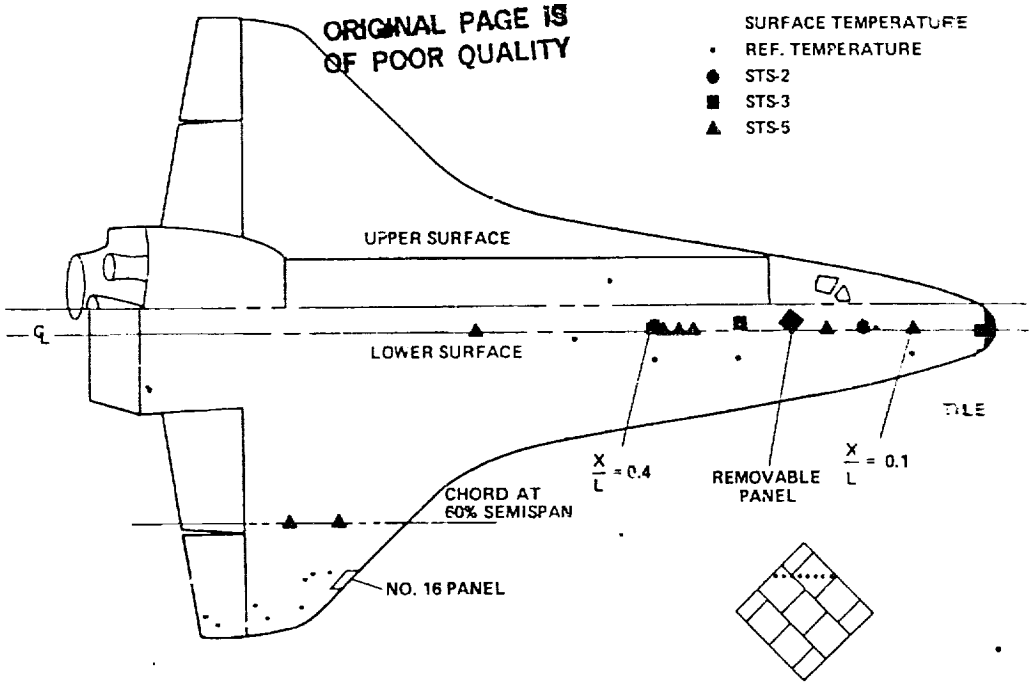

Figure 1.- Experiment thermocouple locations.

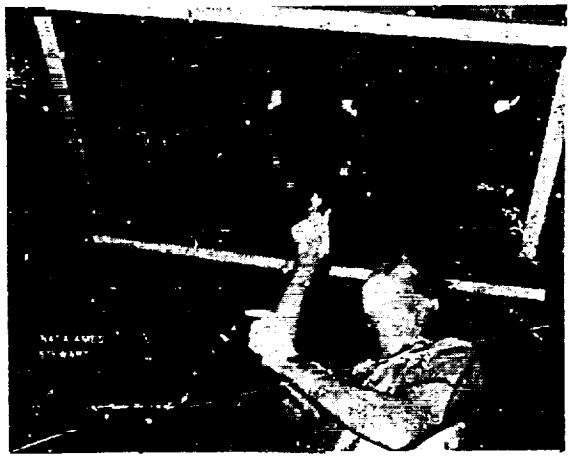

Figure 2.- Catalytic overcoat application.

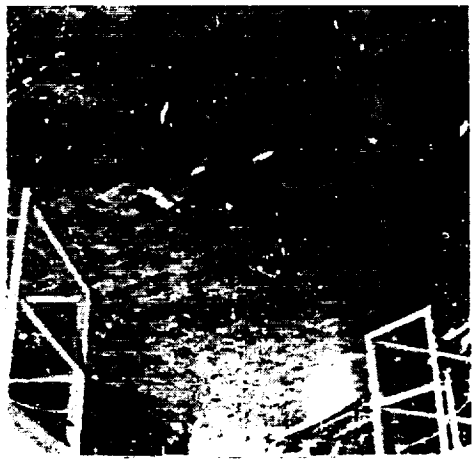

Figure 3.- Preflight STS-5 photograph of experiment.

X/L = 0.1

STRIP, 0.35 ≤ X/L ≤ 0.4

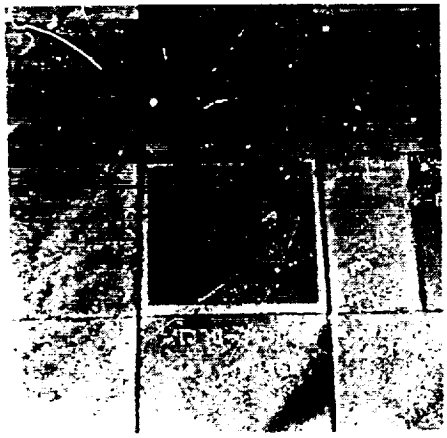

X/L = 0.6

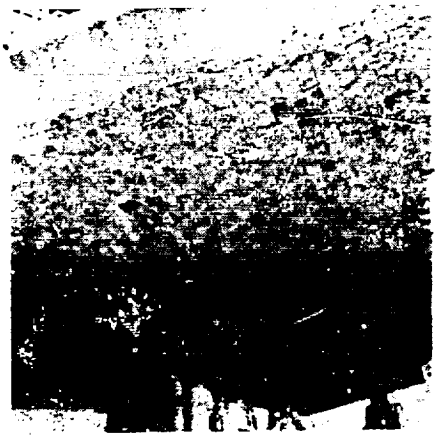

WING, 60% CHORD

Figure 4.- Post-flight STS-5 photograph of selected tiles.

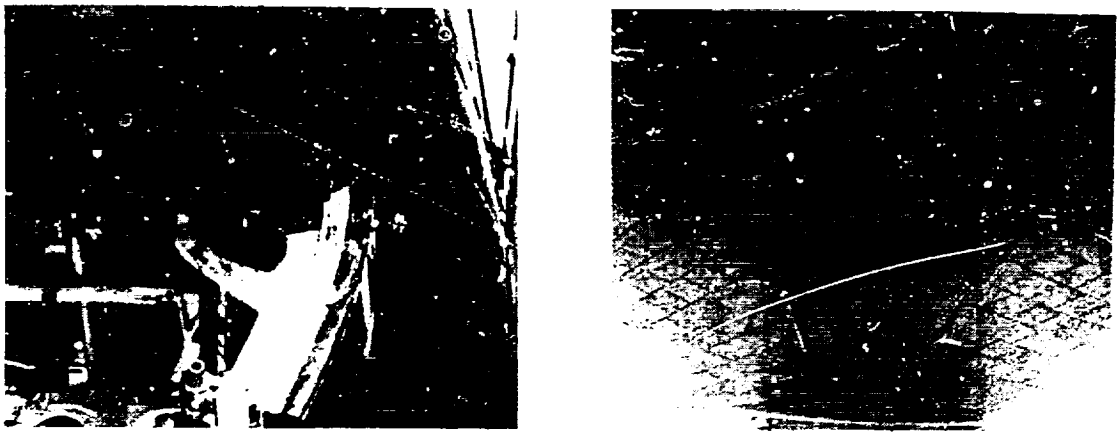

Figure 5.- Contamination sources.

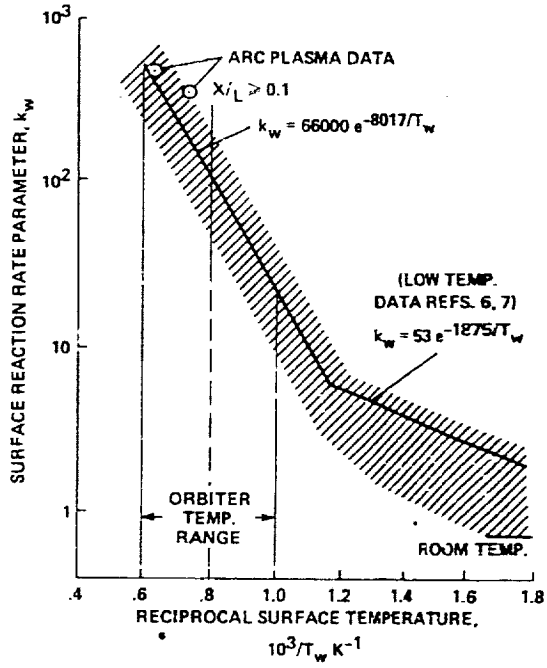

Figure 6.- Initial catalycity of RCG coating.

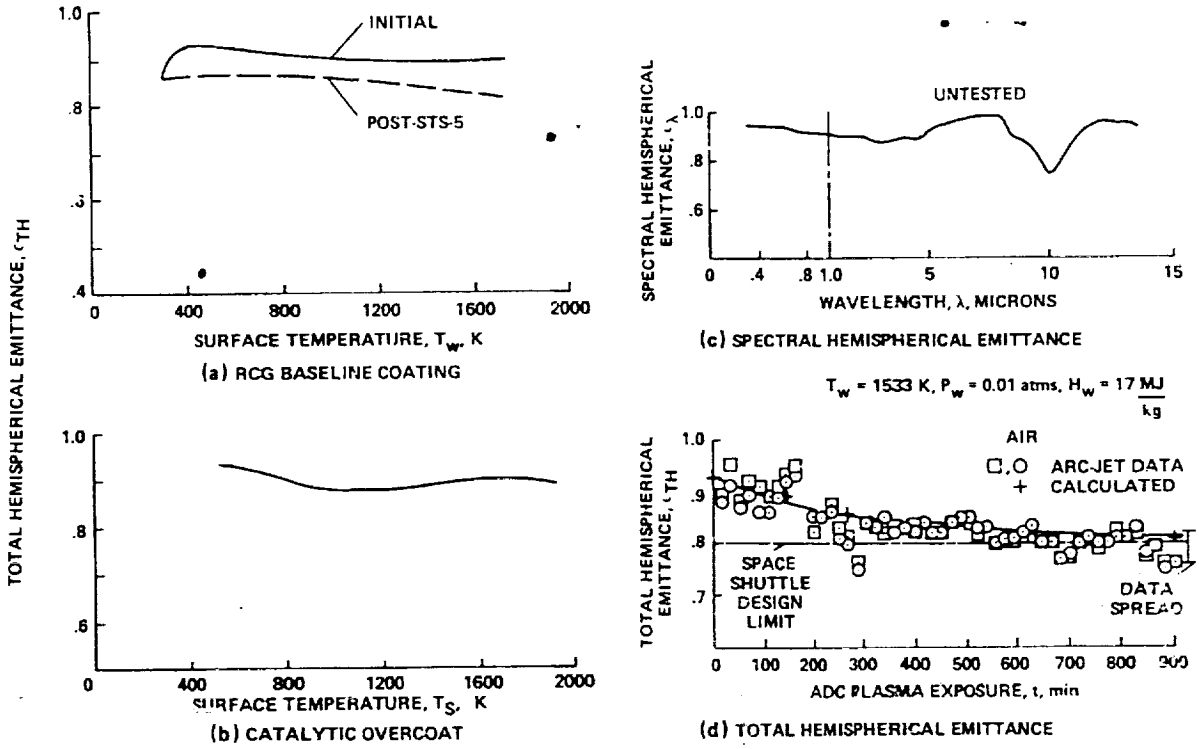

Figure 7.- Hemispherical emittance.

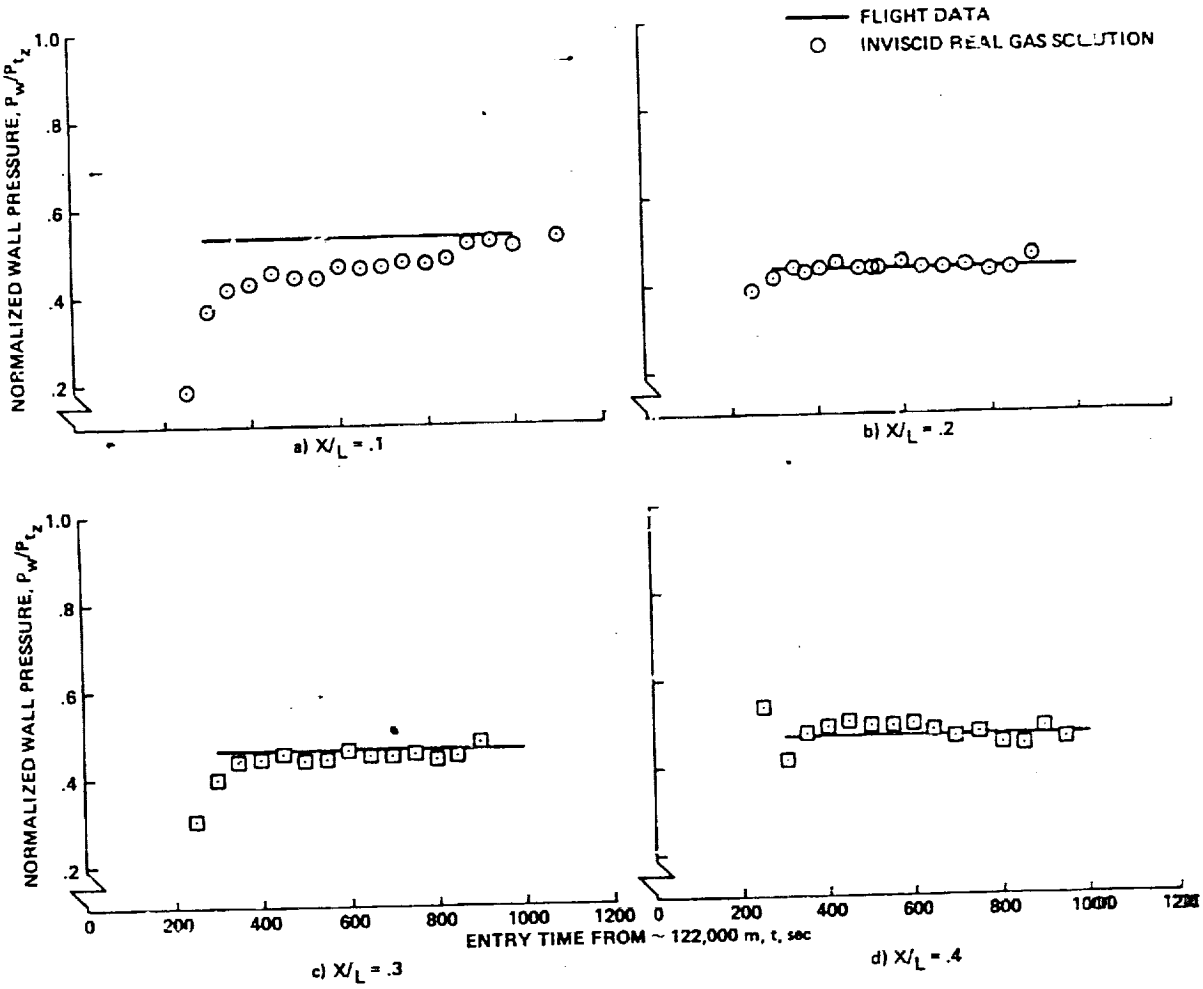

Figure 8.- Pressure histories for flight STS-3 windward centerline.

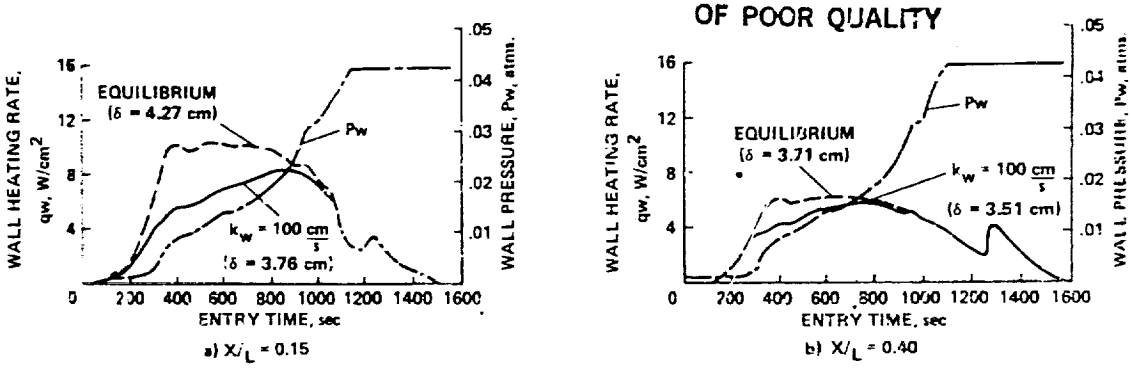

Figure 9.- Calculated STS-3 heating and pressure profiles during entry.

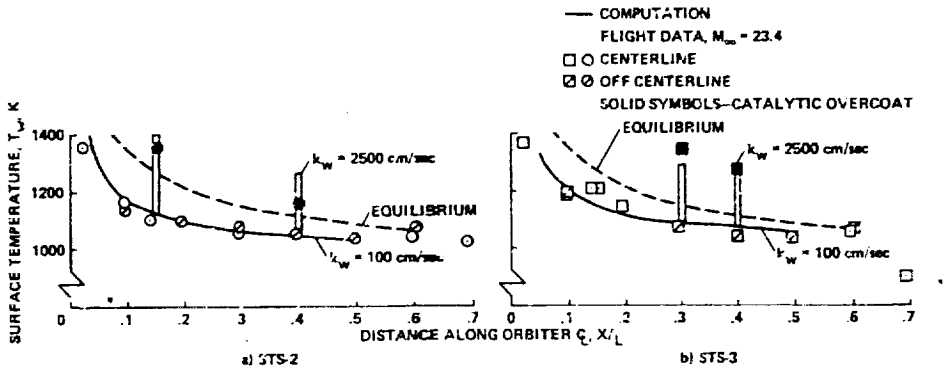

Figure 10.- Surface temperature variation on orbiter windward centerline.

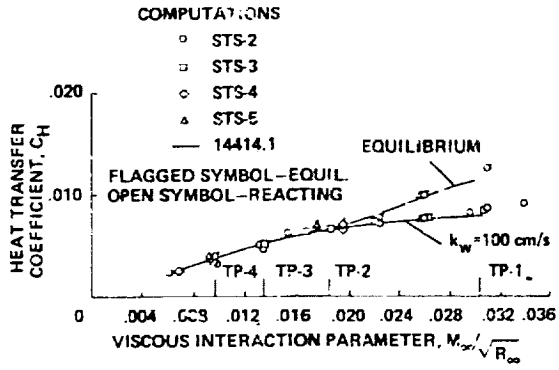

Figure 11.- Correlation of calculated heating transfer coefficients.

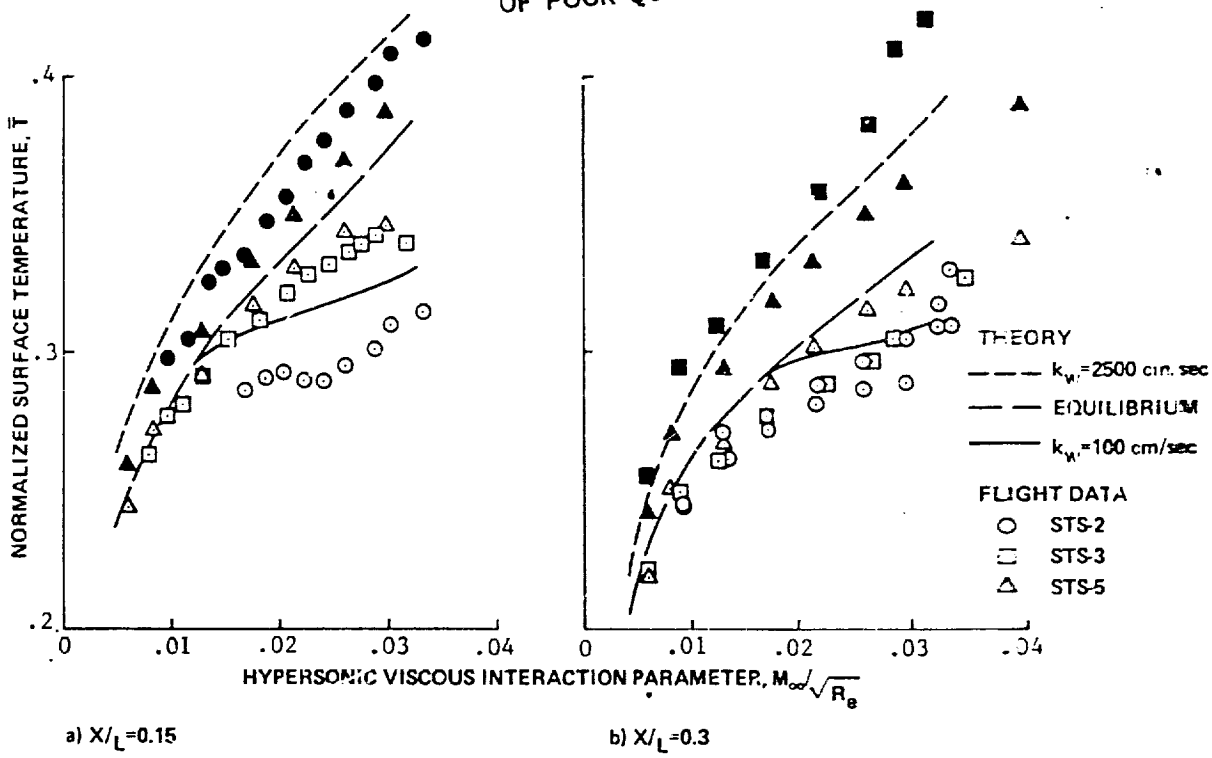

a) $X/_L$=0.15

b) $X/_L$=0.3

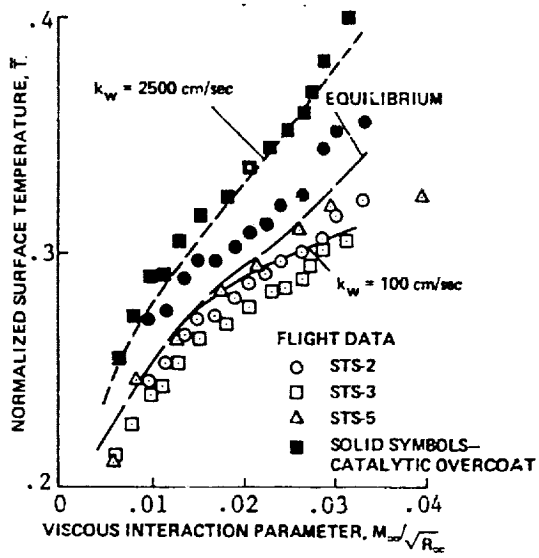

c) $X/_L$=0.4

Figure 12.- Normalized surface temperature as a function of correlation parameter.

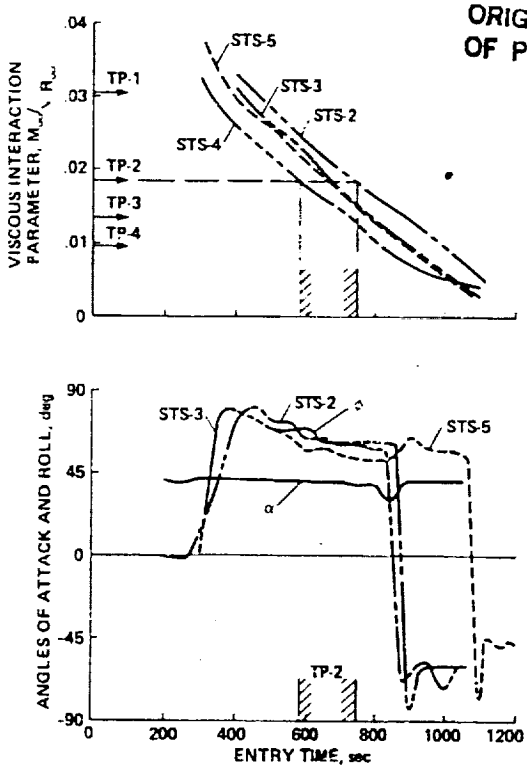

Figure 13.- Flight trajectory parameters.

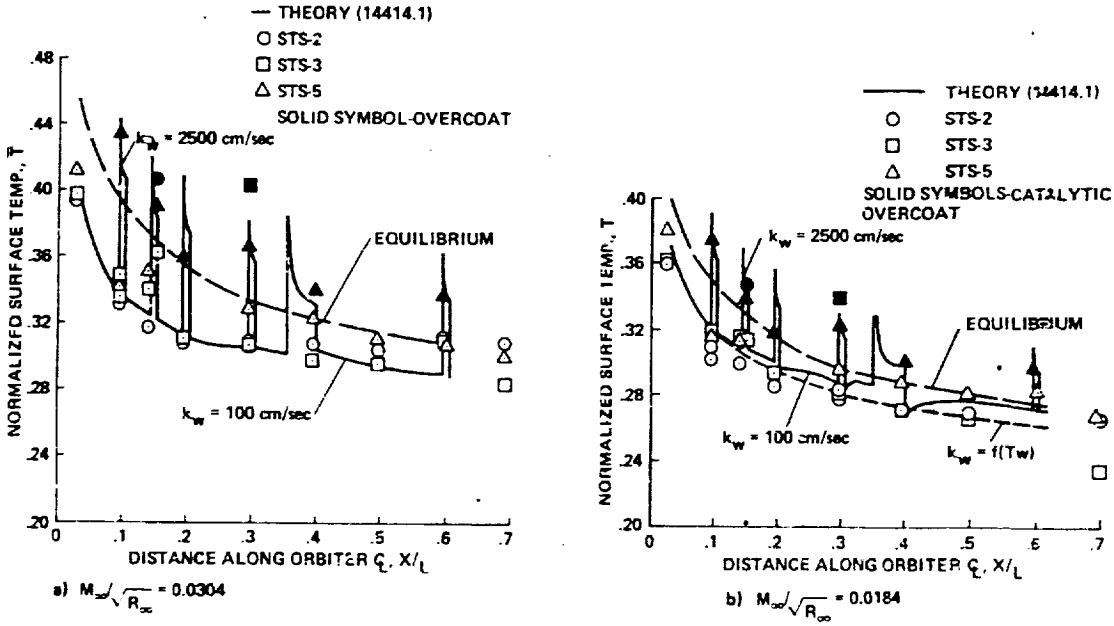

Figure 14.- Surface temperature distribution along midfuselage centerline.

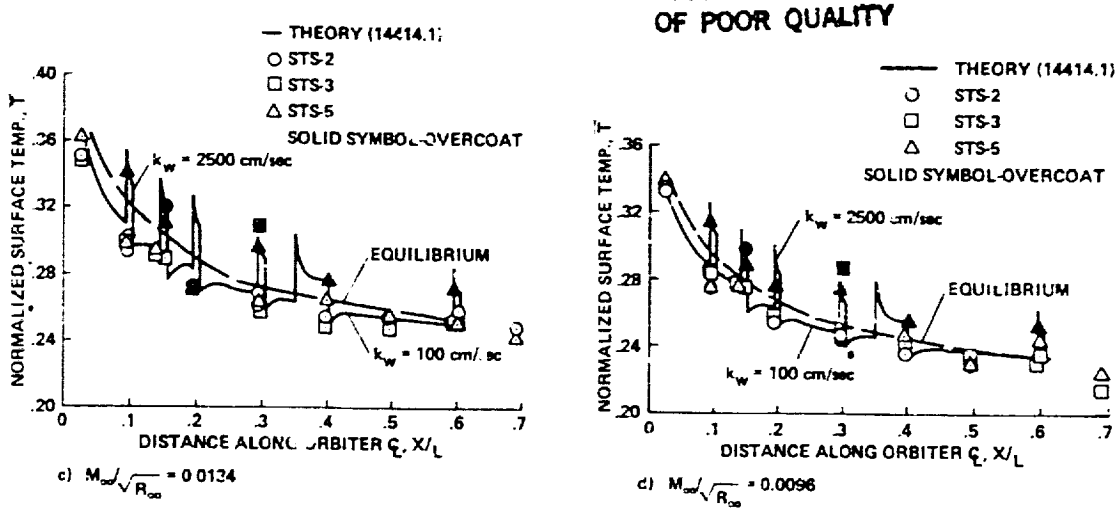

Figure 14.- Concluded.

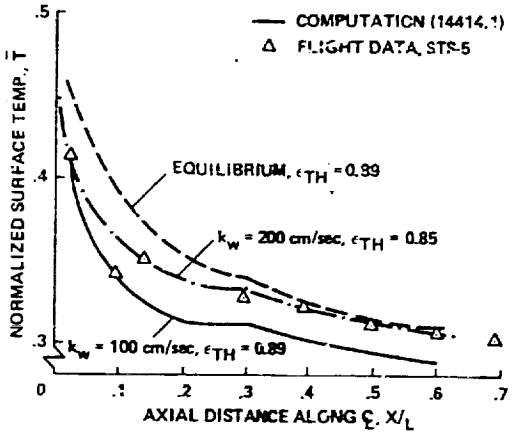

Figure 15.- Comparison between measured and predicted surface temperatures using post-flight STS-5 RCG surface properties.

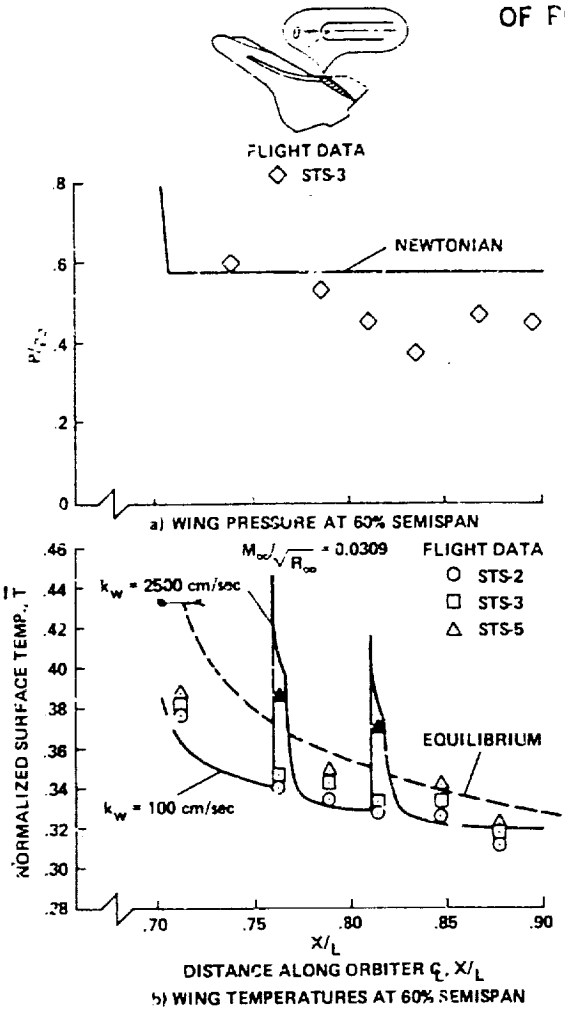

Figure 16.- Surface pressure and temperature distributions along 60% semispan on orbiter wing.